FILOMAT (Niš) 9:3 (1995), 753–764
Algebra, Logic & Discrete Mathematics
Niš, April 14–16, 1995.

DISCRETE METHODS FOR VISUALIZING FRACTAL SETS

Ljubiša M. Kocić

ABSTRACT. A short summary of some known discrete visualizig models of fractal sets is given. A new algorithm, called graphical erosional algorithm, for visualising fractal sets from $\mathbf{R}^2$ is presented. Input parameters for the algorithm are functions from a hyperbolic iterated system. Beside visualizing, this algorithm permits estimation of fractal dimension for a set being visualized.

1. Introduction

The set of points from $\mathbf{R}^2$, defined by $S = \{(x_i, y_i), i = 1, \ldots n_x, j = 1, \ldots n_y,\ n_x, n_y \in \mathbf{N}\}$ will be referred as *the picture support*. Let P be an arbitrary set such that $2 \leq Card(P) \leq n_c (\in \mathbf{N})$ and $\varphi : S \to P$ be any mapping. Then P is called *set of colors* and φ is *color function*. Under *discrete visualization* of an arbitrary set A one assumes the map $\phi : A \to S$, with a given color function ϕ. The triple (ϕ, S, φ) will be called a *discrete visual model* of A.

Discrete visual models are important for processing information by computer, especially when the plane set A has a complicated form, for example, when it is a fractal set or a chaotic attractor, like those in Figure 1. Actually, this figure illustrates orbits of two different dynamical systems. Namely, let $(\mathbf{X}, d)$ be a metric space and $f : \mathbf{X} \to \mathbf{X}$ be an arbitrary mapping. Then, $(\mathbf{X}, f)$ is a *dynamical system*. For any $x_0 \in \mathbf{X}$, the sequence $\{x_i\}_{i=0}^{+\infty}$, such that $x_{i+1} = f(x_i)$ is called the *orbit* of the point x_0. The limit of an orbit

This research was partly supported by Science Fund of Serbia, grant number 0401F, through Matematički institut SANU

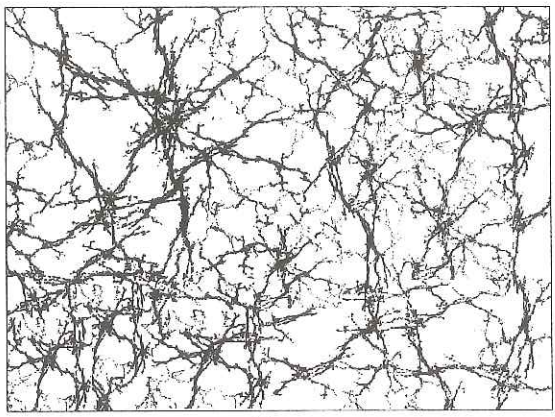

A)

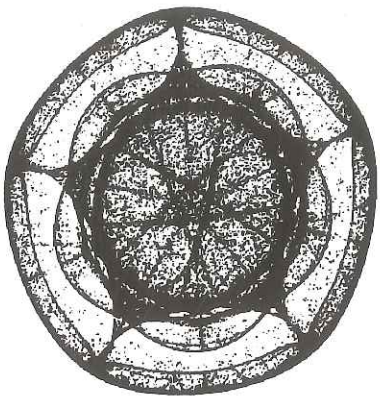

B)

FIGURE 1. A) NEURAL NETWORK AS FRACTAL SET; B) PENTAGONAL CHAOTIC ATTRACTOR OF CHOSSAT-GOLUBITSKY MAPPING

can be a set A in $\mathbf{X}$ which "attracts" an orbit, so it is called *attractor* of dynamical system. In fact, the attractor

$$A = \lim_{n \to +\infty} x_n \ , \quad A \in \mathbf{X} \ ,$$

is a fixed point of the mapping f and it does not depend on x_0. Interesting attractors usually have noninteger Hausdorf dimension, wherefrom the term "fractal" roots its name [5].

Example 1.1. Consider the mapping $f : \mathcal{H}\mathbf{R}^2 \to \mathcal{H}\mathbf{R}^2$ ($\mathcal{H}\mathbf{X}$ is the partitive set of $\mathbf{X}$), such that $f = f_1(B) \cup f_2(B)$, for any $B \subset \mathbf{R}^2$, where f_1 and f_2 are affine plane transformations defined by

$$\begin{aligned} f_1 &: \begin{pmatrix} x \\ y \end{pmatrix} \mapsto \begin{pmatrix} 0.1 & -0.7 \\ 0.7 & 0 \end{pmatrix} \begin{pmatrix} x \\ y \end{pmatrix} + \begin{pmatrix} 0 \\ -1 \end{pmatrix} \ , \\ f_2 &: \begin{pmatrix} x \\ y \end{pmatrix} \mapsto \begin{pmatrix} -0.3863 & 0.1562 \\ -0.3562 & -0.6863 \end{pmatrix} \begin{pmatrix} x \\ y \end{pmatrix} + \begin{pmatrix} 0.4 \\ 0.4 \end{pmatrix} \ . \end{aligned} \tag{1.1}$$

The attractor A of the dynamical system $(\mathcal{H}\mathbf{R}^2, f)$ has the form of a neural cell (see Figure 5). By simple affine transformations of A the model of neural network, a fragment of neural tissue, displayed in Figure 1-A), is obtained.

Example 1.2. Let $\mathbf{C}$ be a complex plane and $f : \mathbf{C} \to \mathbf{C}$ be a mapping given by

$$f(z) = z(z^9 + 4z\overline{z} + \overline{z}^9 - 2.6) + \overline{z}^8 \ . \tag{1.2}$$

The orbit of the point $z_0 = 0$ tends to the attractor of dynamical system $(\mathbf{C}, f)$ shown in Figure 1-B). The mapping (1.2) is known as Chossat-Golubitsky formula [3], [6].

In these examples, two different algorithms are used for creating visual models of corresponding attractors. In both of them, the formula (1.1) or (1.2) are treated like continued expressions, but in computer enviroment, earlier or later, they are rounded off and the discrete values are used for creating visual model. In the next section, several methods that uses discrete tools for creating fractal visual models.

2. Discrete fractal structures

Hausdorf dimension is the most important number connected with a fractal attractor. It offers an estimation how "dense" this attractor occupies the metric space in which it is immerged. For an arbitrary $A \subset \mathbf{X}$, the *Hausdorf dimension** is defined by

$$D_H(A) = \inf_{\mu(A,p)=0} \{p\},$$

where, for $p \in \mathbf{R}$, $p \mapsto \mu(A, p)$ is the *Hausdorff p-dimensional measure* of A

$$\mu(A, p) = \sup_{\varepsilon>0} \{\inf \{\sum_{i=0}^{+\infty} |K_i|^p\}\} .$$

Infimum is taken over all ε-covers $\mathcal{K} = \{K_i\}_{i=0}^{+\infty}$ of A. In the above formula, $|K_i|$ stands for the diameter of $K_i \subset \mathbf{X}$.

Example 2.1. Let consider the Pascal's triangle of binomoal coefficients [8]. Select these elements $p_{n,k} = \binom{n}{k}$ for which $p_{n,k}$ *mod* $2 = 1$ to obtain the set A. Choose the set of colors $I' = \{white, black\}$, and map A in the picture support S by replacing each element of A by a black point (see Figure 2). The visual model of A recognizes as a famous Sierpinski triangle. As it is shown in [8], Hausdorf dimension of A is $D_H = \log_2 3 = 1.58496...$ which is known to be the dimension of Sierpinski triangle [5].

Example 2.2. Many biological object possesses typical fractal properties. One of them, the neural tisue, is mentioned in Figure 1. Another one is the DNA chain, very important natural pattern that conways genetic information. DNA has a form of a double helix being composed of two strands that bind together by a specific base-pairing rule. *Adenine* (A) always pairs with

*Also known as *Hausdorf-Besicovitch* or *geometric* dimension

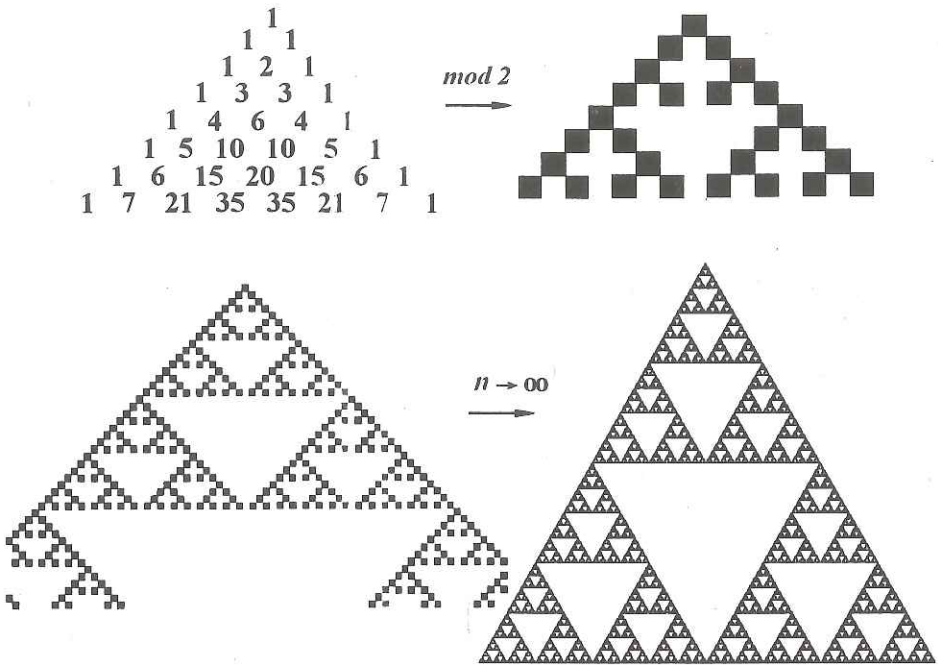

FIGURE 2. BINOMIAL COEFFITIENTS MOD 2 FORM THE SIERPINSKI TRIANGLE

thymine (T) whilst *cytosine* (C) always pairs with *guanine* (G), like in this fragment

$$\begin{array}{ccccccccccccccccccc} - & A & A & C & T & G & G & G & A & T & A & T & A & T & T & T & G & G & G & - \\ & | & | & | & | & | & | & | & | & | & | & | & | & | & | & | & | & | & \\ - & T & T & G & A & C & C & C & T & A & T & A & T & A & A & A & C & C & C & - \end{array}$$

Each DNA strand can be connected with a Brownian motion path as follows: the pair AT corresponds to a particle being moved forward the x-axis for a given step. TA combination moves the particle in the oposite sense for the same step. CG and GC pair moves the particle along the y-axis or in the opposite direction. Alternation AC or CA with GT or TG directs along the $[(0,0)(1,1)]$ vector and the contrary, while AG/GA followed by CT/TC moves the particle along $[(0,0)(-1,-1)]$ or back.

Experiments, done by authors of [2], show that amino-bases of DNA, taken from GenBank has $D_H = 1.631 \pm 0.137$ which is significantly lower than Hausdorf dimension of the curve being a trajectory of a Brownian motion, which is $D_H = 2$. Figure 3 shows the path of Brownian motion (A) and the pseudorandom walks of two DNA (B) and (C).

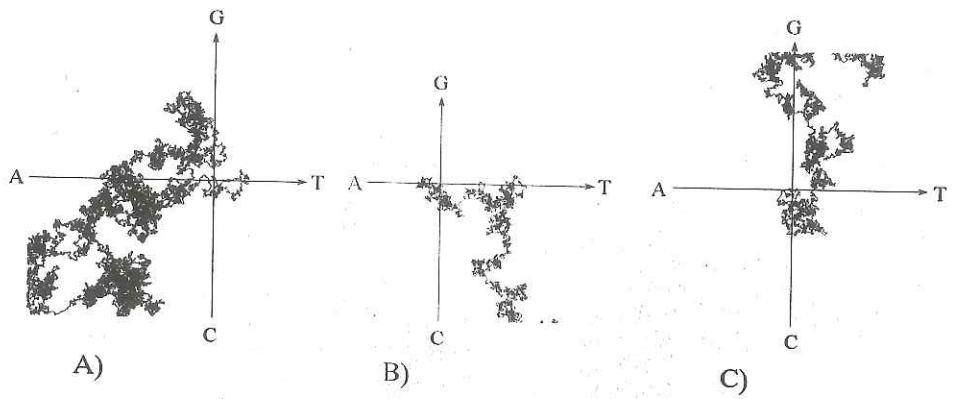

FIGURE 3. A) BROWNIAN MOTION, $H_D = 2$; B) DIMER OPSIN GENE, $D_H \approx 1.744$; C) ALPHA-1-GLYCOPROTEIN, $D_H \approx 1.671$

Example 2.3. Another discrete method for visualizing fractal sets is connected with tilling-patterns. Again start with genetic sequence of DNA taken from the human immunodeficiency virus type 1 (AIDS), and associate the Escherian* tile pattern shown in Figure 4-A) (above) in different orientation, depending on the letter A,T,C or G in the strand. An Escher-like tile is obtained (Fig. 4-A) bellow). Number of closed diamonds in the pattern, divided by the number of tiles, so called *diamond fraction*, characterize the randomnes of the data. If this fraction is about 0.05, the data are randomly distributed. Correlation appears if the fraction tends to zero.

Another type of patern, shown in Figure 4-B) is called Truchet patern, after Sebastian Truchet that studied such patterns in his paper from 1704. Diamond fraction is now replaced by the *dumbell fraction* which makes about 0.0125 for the random data. Increasind diagonal trend in the pattern reveals increasing correlation of the data. For more details see [6].

3. Graphical erosional algorithm

One of the most suitable ways to define and produce fractal sets is by (hyperbolic) Iterative Function System (IFS). This is a collection of contractive maps $(f_1, \ldots, f_n)$ that act in a metric space $(\mathbf{X}, d)$, i.e. $W = \{\mathbf{X}, f_1, \ldots, f_n\}$. The Lipschitz factor of W is $s = \max_i\{s_i\}$, where s_i is the contractive factor of f_i. Then, there exists a unique attractor A such that $A = F(A)$, where $F = \cup_{i=1}^{n} f_i$, the assertion known as the Hutchinson theorem. In other words, $A \in \mathcal{H}\mathbf{X}$ is a fixed point for the dynamical system $(\mathbf{X}, F)$.

*after Mauritus Cornelis Escher (1898–1971), duch artist

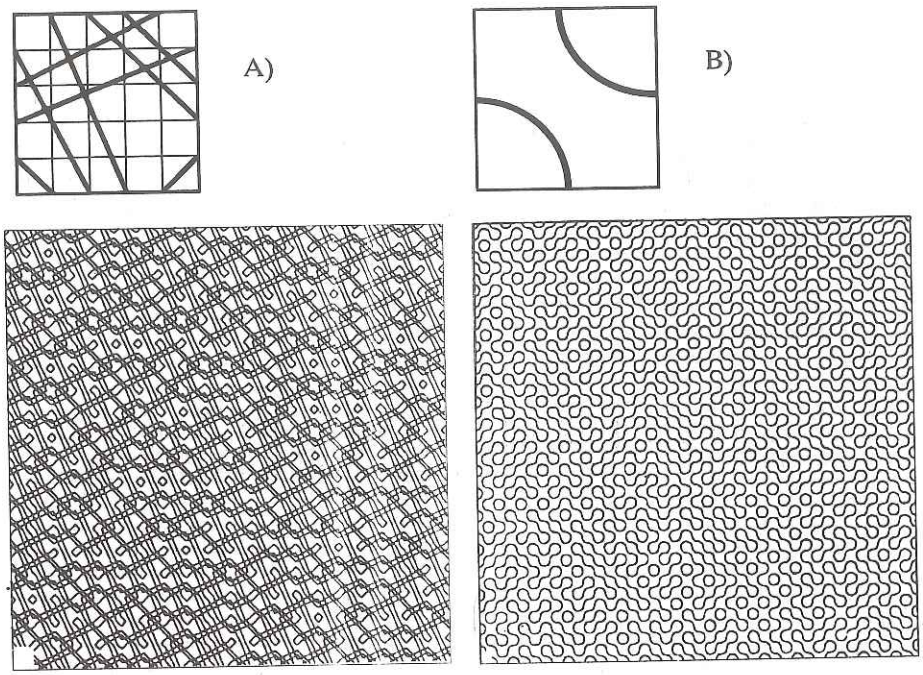

FIGURE 4. A) ESCHER-TILE OF RANDOM DATA (ESCHERGRAM); B) TRUCHET-TILE OF RANDOM DATA

According to the literature ([4]), there are five different algorithms for calculating (and therefore for visualizing) fractal attractors in $(\mathbf{R}^2, d)$.

Algorithm A. *Based on the Hutchinson theorem, this algorithm starts with an arbitrary closed subset B from $\mathbf{R}^2$ and transforms it by F. More precisely,*

a) initialize $B_0 \in \mathcal{H}(\mathbf{R}^2)$,

b) calculate $B_{k+1} = \cup_i f(B_k)$, $k = 0, 1, \ldots$,

c) apply a discrete visualization $\phi : B_k \to B_k^s$.

Repeat b) and c) until $h(B_k^s, B_{k+1}^s) < \varepsilon$, where h is Hausdorff metric and ε is the minimal distance between points in the picture support (picture norm).

Good results are gain by choose B_0 to be a singleton, typically a fixed point of one of contractions f_i from IFS.

Algorithm B (Barnsley, Demko). *This algorithm uses a sequence of independent random variables $\{\varphi_j\}_{j \in \mathbf{N}}$, such that $pr(\varphi_j = f_i) > 0$ for any j and $i = 1, \ldots n$.*

a) Choose $r_0 \in \mathbf{R}^2$,

b) calculate $r_k = \varphi(x_{k-1})$, $k = 0, 1, \ldots$,

c) map each r_k onto the picture support.

Repeat b) and c) until the Hausdorff distance between two consecutive pictures become smaller than the picture norm.

The following three algorithms are given by Dubuc and Elqortobi [4].

Algorithm C (Based on Williams formula). *Let W^* be the set of all finite compositions of functions of W. Let for $g \in W^*$, $Fix(g)$ denotes the fixed point of g. Williams in* [7] has shown that the closure of $\cup_{g \in W^*} Fix(g)$ is invariant and there is no other closed bounded invariant sets for F.

Let $\varepsilon > 0$ and $W(\varepsilon)$ be a family of contractions. A function g is in $W(\varepsilon)$ if there is a finite sequence of functions of W, $f_1, f_2, \ldots, f_n$, such that:

(1) g is the composition $f_1 \circ f_2 \circ \cdots \circ f_n$ and the Lipschitz constant of g is $\leq \varepsilon$.

(2) If $k < n$, then the Lipschitz constant of $f_1 \circ \cdots \circ f_k$ is larger than ε.

Then the set $B = \{Fix(g) : g \in W(\varepsilon)\}$ is an approximation of A.

Algorithm D. *This is a variant of the Algorithm C. The attractor A is approximated by $B = \{h \circ R \circ g(x), h \in W(\varepsilon)\}$, where R is a rounding map of the metric space* $\mathbf{X}$.

Algorithm E (Graphical algorithm). *Let δ be a positive real number, and $M(\delta)$ be a subset of* $\mathbf{X}$ *such that*

(a) for any x in $\mathbf{X}$, $d(x, M(\delta)) < \varepsilon$;

(b) in any ball of $\mathbf{X}$, *there is just a finite number of points of $M(\delta)$.*

Let B_n and C_n are two sequences of subsets of $\mathbf{X}$ *for $n = 0, 1, \ldots$. Then,*

(1) *A point x is choosen in C_n;*

(2) *A temporary set T is initially empty. A loop over W is done, such that for each $f \in W$ for which $d(f(x), B_n \cap T) \geq \delta$, one chooses a point $x' \in M(\delta)$, such that $d(f(x), x') < \delta$, and is added to T.*

(3) $B_{n+1} = B_n \cup T$ *and* $C_{n+1} = C_n \cup T \backslash \{x\}$.

Probably the most important quantity connected with the fractal set is its dimension. There are many definitions of dimensions, but the way of calculating them may be an awquard question. The most popular method for experimental estimating the fractal dimension of an attractor in $\mathbf{R}^2$ is the box-counting method, which is based on the following theorem [1]:

Theorem 1 (Box Counting Theorem). *Let $A \in \mathcal{H}(\mathbf{R}^2)$, and Euclidean metric is used. Tile the plane $\mathbf{R}^2$ by the square uniform mesh with the step 2^{-n}. Let $\mathcal{N}_n(A)$ denote the number of boxes from the mesh that intersect the attractor. If*

$$D_H = \lim_{n \to \infty} \left\{ \frac{\ln \mathcal{N}_n(A)}{\ln(2^n)} \right\}, \tag{2.1}$$

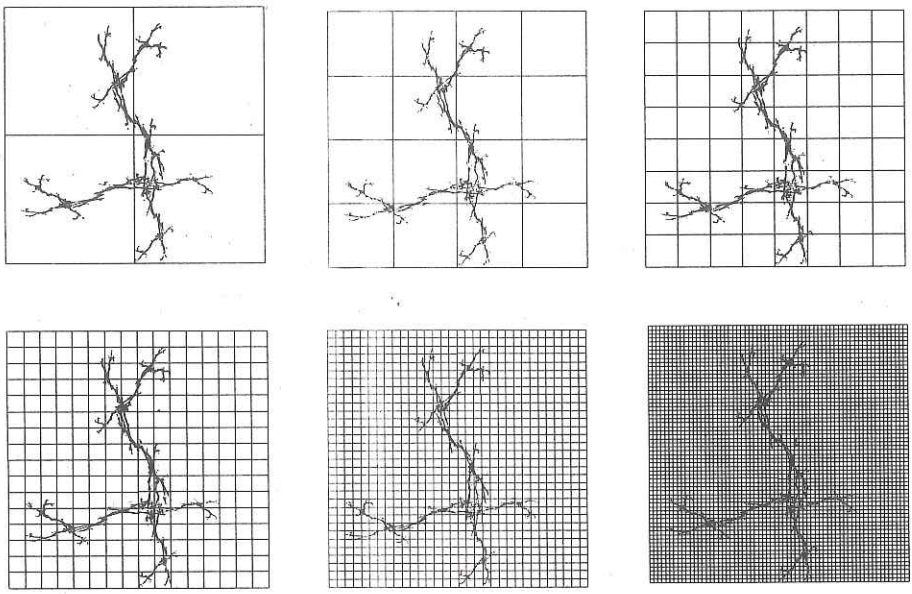

FIGURE 5. A "NEURAL CELL" AND THE BOX COUNTING METHOD

exists, then A has fractal dimension D_H.*

The graphical erosional algorithm which will be described bellow, gives succesive approximations of fractal sets in $\mathbf{R}$ and calculates an approximation of its fractal dimension at same time.

Actually, let M_n be a uniform mesh as described in Theorem 1. Note that the scale plays no role in calculating D_H from (2.1). So, for a unit of measure one can take the side of a square that "nicely" framed the set A. Figure 5 shows a fractal attractor that resembles to the neural cell. It is framed by an apropriate square M_0 with the side lenght 1. It is divided into four subsquares which corresponds to the net M_1 (the upper left square in Figure 5). The process continues for $n = 3, 4, 5, 6$. Let $K_n(A)$ denotes 2^{-n}-cover of A. The following algorithm produces sets $K_n(A)$ and calculate the fractal dimension at the same time.

Graphical Erosional Algorithm (GEA). *Let $n \in \mathbf{N}$. The set of nodal points $\{(i/2^n, j/2^n)\}$ from $\mathbf{R}^2$ determines the standard orthogonl net M_n. Let $\Delta^n_{i,j}$ be a cell of M_n, i.e. the set of points (x, y) such that $i/2^n \leq x <$*

*also called *box dimension*

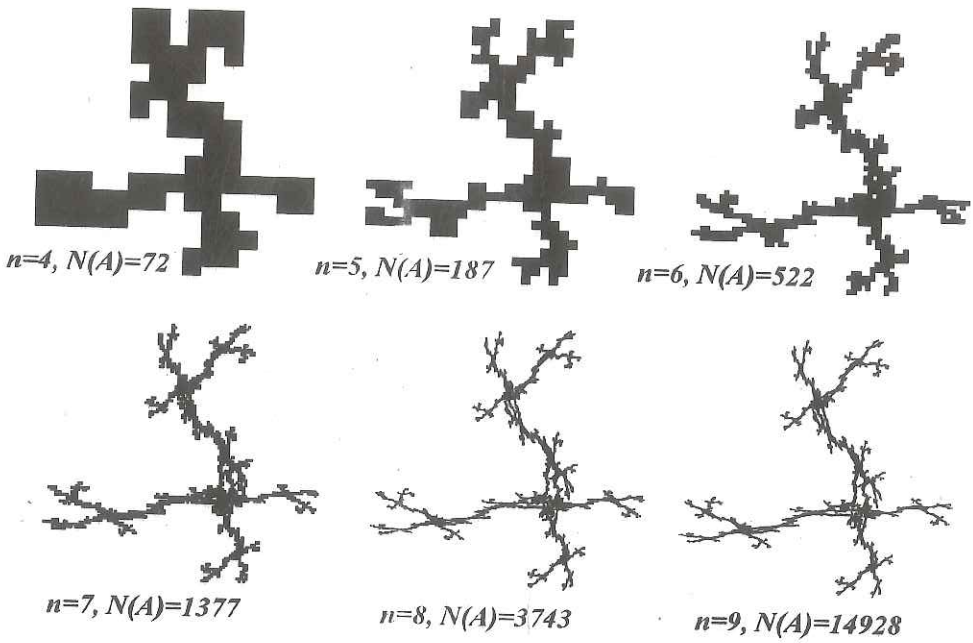

FIGURE 6. GRAPHICAL EROSIONAL ALGORITHM

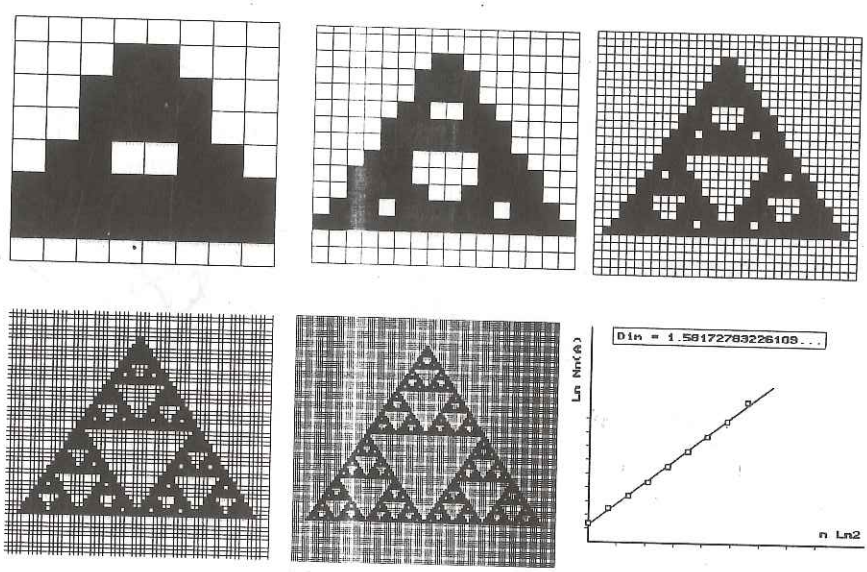

FIGURE 7. TESTING OF GRAPHICAL EROSIONAL ALGORITHM

$(i+1)/2^n$ *and* $j/2^n \le y < (j+1)/2^n$. *Let* $S \in \mathbf{R}$ *be the picture support with the norm* $\delta(S) = \max\{d(x_i, x_{i+1}),\ d(y_j, y_{j+1})\}$, *and* $P = \{black, white\}$ *be the set of colors. For any IFS, say* $W = \{\mathbf{R}, f_1, \ldots, f_m\}$ *with the attractor* A, *the sequence of color functions* $\phi_n : A \to S$ *is associated with the net* M_n *according to the following steps:*

(1) *Initialize* $n = 1$ *and* $\mathbf{R} \leftarrow \{white\}$;

(2) *Produce the point* $p_k = (x_k, y_k)$ *by the Barnsley-Demko algorithm;*

(3) *If* $p_k \in \Delta^n_{i,j}$, *then* $\tilde{K}_n = S \cap \Delta^n_{i,j} \to \{black\}$;

(4) *Count the number* $\mathcal{N}_n(A)$ *of* Δ^n*-cells in* K_n;

(5) $n \leftarrow n+1$. *If* $\delta(S) > 2^{-n}$ *then go to* (1), *otherwise go to* (6).

(6) *Calculate an approximation value of* D_H, *given by* (2.1), by fitting the data $\{(\ln(2^n), \ln \mathcal{N}_n(A))\}$ by a least-square affine function. The coefficient of the linear term is D_H. $D_H \approx \tan\alpha$.

This algorithm is illustrated in Figure 6 with A being a neural cell from Fig. 5. Note that the 'black' set, $\tilde{K}_n$, generated in step 3 approximates 2_n-covers of A. The number of black squares is denoted by $N(A)$.

Then the following theorem supports the algorithm:

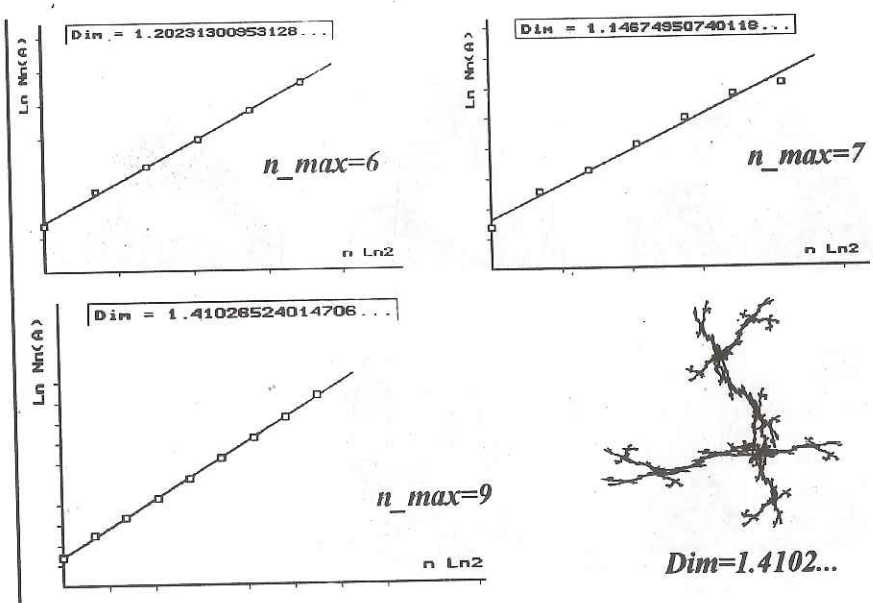

FIGURE 8. DIMENSION "BY HANDS' AND BY GEA

Theorem 2. *If $\delta(S) \to 0$ and $n \to \infty$, then the sequence $\{\tilde{K}_n\}_{n=1}^{\infty}$, generated by the GEA converges to A, in Hausdorff metric.*

Proof. Denote the Hausdorff distance between two sets X and Y from $\mathbf{R}^2$ by $h(X,Y)$. Suppose that this metric is induced by the Euclidean metric in $\mathbf{R}^2$. It is obvious that

$$h(S,A) \leq \frac{\sqrt{2}}{2}\delta(S)\ . \tag{3.1}$$

Let $r_k = (x_k, y_k)$ be the point produced by the Algorithm B. If $r_k \in \Delta_{i,j}^n$ then the cell $\Delta_{i,j}^n$ becomes a part of $K_n(A)$. As $h(r_k, \Delta_{i,j}^n) \leq \sqrt{2}2^{-n}$, then

$$h(K_n(A), A) \leq 2^{-n+\frac{1}{2}}\ , \tag{3.2}$$

As by definition, $\tilde{K}_n(A) = K_n(A) \cap S$, then by (3.1) and (3.2)

$$h(\tilde{K}_n(A), A) \leq \frac{\sqrt{2}}{2}(2^{-n+1} + \delta(S))\ .$$

Thus, if $n \to \infty$ and $\delta(S) \to 0$ then $h(\tilde{K}_n(A), A) \to 0$, in Hausdorff metric.

Note that the proof holds if the Euclidean metric is replaced by any other metric in $\mathbf{R}^2$.

Calculation of fractal dimension follows from Theorem 1.

Since the algorithm constructs succesive $1/2^n$-covers of A, it resembles the process of erosion, which suggests the name. Algorithm is tested through several examples. Here, the results of applying GEA on Sierpinski triangle fractal attractor is shown in Figure 7. The estimated fractal dimension is 1.5817... which approximates the true dimension 1.58496... with accuracy 10^{-2}, which is a good result for PC computer where n can not exceed 9.

Fractal dimension of the "neural cell" is estimated to be 1.4102.... The data and the fitting line are shown in Figure 8 (left-bellow). Comparing with box-counting performed "by hands" for $n \leq 6$ and $n \leq 7$ (same figure, above), the data produced by GEA are much more regularly placed along the line. Note that accuracy fails for $n = 7$ due to the weakness of the human eye.

The GEA has one more advantage. It can be used for the rough estimation of the fractal attractor's shape, its dimensions and location in $\mathbf{R}^2$.

References

[1] M. F. Barnsley, *Fractals Everywhere*, Academic Press, 1988.
[2] C. L. Berthelsen, J. A. Glazier, M. H. Skolnick, *Global fractal dimension of human DNA sequences treated as pseudorandom walks*, Phys. Rew. A **45** (1992), 8902–8913.
[3] P. Chossat, M. Golubitsky, *Symmetry-increasing bifurcations of chaotic attractors*, Physica D **32** (1988), 423–426.
[4] S. Dubuc, A. Elqortobi, *Approximation of fractal sets*, J. Comput. Appl. Math. **29** (1990), 79–89.
[5] B. B. Mandelbrot, *The fractal geometry of nature*, Updated and augmented, W. H. Freeman, New York, 1983.
[6] C. A. Pickover, *Mathematics and beauty: Several short classroom experiments*, Notices AMS **38** (1991), 192–196.
[7] R. F. Williams, *Composition of contractions*, Bol. Soc. Brasil. Mat. **2** (1971), 55–59.
[8] S. Wolfram, *Geometry of binomial coefficients*, Amer. Math. Monthly **91** (1984), 566–570.

Department of Mathematics, Faculty of Electronic Engineering, P.O.Box 73, 18000 Niš